SEMI-SUPERVISED CLASSIFICATION OF POLARIMETRIC SAR IMAGES USING MARKOV RANDOM FIELD AND TWO-LEVEL WISHART MIXTURE MODEL

Chi Liu[1,2], Wenzhi Liao[1], Heng-Chao Li[2], Rui Wang[2] and Wilfried Philips[1]

[1] TELIN-IPI, IMEC-Ghent University, Ghent, Belgium
[2] Sichuan Provincial Key Laboratory of Information Coding and Transmission, Southwest Jiaotong University, Chengdu 610031, China

ABSTRACT

In this work, we propose a semi-supervised method for classification of polarimetric synthetic aperture radar (PolSAR) images. In the proposed method, a 2-level mixture model is constructed by associating each component density with a unique Wishart mixture model (instead of a single Wishart distribution as that in the conventional Wishart mixture model). This modeling scheme facilitates the accurate description of data for the categories, each of which includes multiple subcategories. The learning algorithm for the proposed model is developed based on variational inference and all the update equations are obtained in closed form. In the learning algorithm, the spatial interdependencies are incorporated by imposing a Markov random field prior on the indicator variable to alleviate the speckle effect on the classification results. The experimental results demonstrate the improved performance of the proposed method compared with the unsupervised version and supervised version of the proposed model as well as an existing method for semi-supervised classification.

Index Terms— Polarimetric synthetic aperture radar (PolSAR), semi-supervised classification, finite mixture model, variational inference, remote sensing.

1. INTRODUCTION

Polarimetric synthetic aperture radar (PolSAR) is an advanced imaging system, which actively emits microwave and receives back-scattered signals in horizontal and vertical polarization [1]. With different combinations of emitting and receiving polarization, multi-channel PolSAR images are acquired, which provide rich information about the physical scattering mechanism over the illuminating area and help to better understand observing targets. PolSAR images have been pervasively used in various applications such as ship detection, agriculture monitoring, and environment surveillance.

For the interpretation of PolSAR images, many unsupervised methods have been proposed. In H/α-Wishart methods, all the pixels in a PolSAR image are first assigned to eight categories according to the H/α classification scheme, and then the resulting classification map is further refined by using the Wishart classifier to take into account the statistical property of PolSAR data [2]. Based on this statistical property, the complex Wishart distribution is introduced as the component density of a finite mixture model, leading to a Wishart mixture model (WMM) for unsupervised classification of PolSAR images [3]. The WMM method associates each of its Wishart-distributed components with a unique category. Thus, the labels in the unsupervised classification can be obtained by assigning each pixel to a component according to Bayes' rule. Although the effectiveness of these methods has been verified, they suffer from the unreliable results, which could be either too coarse or over-detailed especially for the interpretation of a large PolSAR image with a great number of categories.

In the aforementioned methods, each category is essentially characterized by a single Wishart distribution. However, this modeling scheme is not always accurate for a complicated category, which generally involves multiple subcategories. For instance, in an urban area, there could be roads, trees, and houses, which statistically exhibit different characteristics from each other. Thus, the inaccurate modeling in the aforementioned methods could lead to the degraded classification performance.

PolSAR images generally exhibit a granular "noise" pattern, which results in a severe "salt-and-pepper" appearance in classification maps of the pixel-wise methods. To improve the quality of the interpretation results, a commonly used technique to incorporate the local correlation is Markov random field (MRF), which effectively models the spatial structure of labels and facilitates the good interpretation of PolSAR images [4,5].

In this paper, we propose a two-level Wishart mixture model (2L-WMM) with a Markov random field prior (2L-WMM-MRF) for semi-supervised classification of PolSAR

images. Within the framework of finite mixture models, the proposed 2L-WMM adopts a unique WMM for each component (category) to describe the mixture of statistical characteristics in each category. The algorithm for semi-supervised learning of the proposed model is developed based on variational inference. In our method, the closed-form update equations are achieved for convenient implementation. The resulting algorithm resembles an iterative procedure that first predicts the labels for the unlabeled samples and then adds all these labels and samples into the training set so as to estimate the parameters for each category. To alleviate the "salt-and-pepper" effect, the local correlations are incorporated by further introducing the MRF prior in the two-level mixture model. The proposed method is tested with a realistic PolSAR image over an agriculture area.

2. PRELIMINARIES

2.1. Statistical properties of PolSAR data

By stacking the back-scattered signals from different polarimetric channels, PolSAR data can be represented as a complex-valued vector $S = [S_{hh}, S_{hv}, S_{vh}, S_{vv}]^T$ [1]. Here, T is the transpose operator. The subscripts for the vector entries indicate the emitting and receiving polarizations, in that order. The multilook covariance matrix is obtained by averaging the neighboring pixels as [1]

$$C = \frac{1}{L} \sum_{i=1}^{L} S_i S_i^H, \qquad (1)$$

where L is the number of looks, and the superscript H is the Hermitian transpose operator. Under fully developed speckle conditions [1], the covariance matrix follows the complex Wishart distribution [6]

$$\mathcal{W}(C; L, \Omega^{-1}) = \frac{L^{Ld}}{\Gamma_d(L)} \frac{|C|^{L-d}}{|\Omega^{-1}|^L} \exp\left\{-L \cdot tr(\Omega C)\right\}, \quad (2)$$

where $\Gamma_d(L) = \pi^{\frac{d(d-1)}{2}} \prod_{i=0}^{d-1} \Gamma(L-i)$, and $\Gamma(x) = \int_0^{+\infty} z^{x-1} \exp\{-z\} dz$ is the Gamma function. d is the number of entries in the vector S. $tr(\cdot)$ and $|\cdot|$ are the trace and the determinant operator, respectively. The complex Wishart distribution has been widely used to construct statistical models for the tasks of interpreting PolSAR images.

2.2. Variational Inference

In variational inference [7], the Bayesian inference is conducted by minimizing the Kullback–Leibler divergence between the true posterior distribution and the approximated posterior distribution $q(\Lambda)$, which is also equivalent to maximizing the variational lower bound $\mathcal{L}(q(\Lambda))$ as [7]

$$\max_{q(\Lambda)} \quad \mathcal{L}(\mathbf{X}, q(\Lambda)) = \int q(\Lambda) \ln \frac{p(\mathbf{X}|\Lambda)p(\Lambda)}{q(\Lambda)} d\Lambda, \quad (3)$$

where $\Lambda = \{\Lambda_i\}$ and $\mathbf{X}$ are the sets of the random variables and the observations, respectively. $p(\Lambda)$ is the joint prior distribution of the all the random variables.

To achieve tractable solutions to the posterior distribution, the factorized approximation is commonly exploited, which restricts the approximated posterior distribution to the form of $q(\Lambda) = \prod_i q_i(\Lambda_i)$. With this approximation, the posterior distribution can be obtained as [7]

$$q^*(\Lambda_i) = \frac{\exp\left\{\mathbf{E}_{j \neq i}[\ln p(\mathbf{X}, \Lambda)]\right\}}{\int \exp\left\{\mathbf{E}_{j \neq i}[\ln p(\mathbf{X}, \Lambda)]\right\} d\Lambda_i}, \quad (4)$$

where $\mathbf{E}_{j \neq i}[\ln p(\mathbf{X}, \Lambda)] = \int \ln p(\mathbf{X}, \Lambda) \prod_{j \neq i} (q_j(\Lambda_j) d\Lambda_j)$.

3. METHODOLOGIES

3.1. Two-Level Wishart Mixture Model

For the modeling problem of multiple subcategories, the density for each component in a finite mixture model (FMM) should be sufficiently flexible to describe the statistical characteristics of the data belonging to a complicated category. To this end, the framework of FMM is used to achieve flexible and accurate models as component densities, leading to a mixture of mixture models (i.e., a two-level mixture model). Thus, by using the WMM as the component densities, we propose a two-level Wishart mixture model (2L-WMM), i.e.,

$$p(C) = \sum_{i=1}^{M} \left(\phi_i \cdot \sum_{j=1}^{K} \omega_{ij} \mathcal{W}(C; L, \Omega_{ij}^{-1}) \right). \quad (5)$$

The introduced WMM component in the proposed model is able to describe a multimodal distribution with great potential in characterizing multiple subcategories. The mixing coefficient ϕ_i is associated with the top-level mixture model. Meanwhile, the mixing coefficient ω_{ij} is associated with the secondary-level mixture model, which helps to model the subcategories.

3.2. Variational Inference for Semi-supervised Learning of the Proposed Model

The proposed 2L-WMM is learned based on the variational Bayes. To derive the variational learning algorithm, the Bayesian inference model is first established by introducing indicator variables and by selecting conjugate prior distributions [7]. Specifically, hidden indicator variables $\mathbf{Z} = \{\mathbf{z}_n\}$ and $\mathbf{Y} = \{\mathbf{y}_{ni}\}$ are introduced respectively for the top and the secondary mixture model. $\mathbf{z}_n = [z_{n1}, z_{n2}, \cdots, z_{nM}]$ and $\mathbf{y}_{ni} = [y_{ni1}, y_{ni2}, \cdots, y_{niK}]$ are binary vectors with only one 1-valued element to indicate which category and subcategory data n belongs to. The multinomial distribution is selected as the distribution for these hidden variables. The prior distributions of the mixing coefficients (i.e., $\Phi = \{\phi_i\}$

and $\boldsymbol{\omega} = \{\omega_{ij}\}$) are assigned with the Dirichlet distributions. The prior distributions for the component parameters (i.e., $\boldsymbol{\Omega} = \{\Omega_{ij}\}$) are selected as the complex Wishart distribution. The complete-data loglikelihood function for the proposed 2L-WMM can be obtained by product rule.

The semi-supervised learning algorithm for the proposed model is developed by maximizing the following objective function, depending on both the unlabeled samples ($\mathbf{C}_{\mathfrak{U}}$) and the labeled samples ($\mathbf{C}_{\mathfrak{L}}$):

$$\max_{q(\boldsymbol{\Lambda})} \int q(\boldsymbol{\Lambda}) \ln \frac{p(\boldsymbol{\Lambda}_2)p^{\lambda_{\mathfrak{U}}}(\mathbf{C}_{\mathfrak{U}}, \boldsymbol{\Lambda}_1|\boldsymbol{\Lambda}_2)p^{\lambda_{\mathfrak{L}}}(\mathbf{C}_{\mathfrak{L}}, \boldsymbol{\Lambda}_1|\boldsymbol{\Lambda}_2)}{q(\boldsymbol{\Lambda})} d\boldsymbol{\Lambda}, \tag{6}$$

where $\boldsymbol{\Lambda} = \{\boldsymbol{\Lambda}_1, \boldsymbol{\Lambda}_2\}$. $\boldsymbol{\Lambda}_1 = \{\mathbf{Z}, \mathbf{Y}\}$ and $\boldsymbol{\Lambda}_2 = \{\boldsymbol{\Phi}, \boldsymbol{\omega}, \boldsymbol{\Omega}\}$ are respectively the set of the introduced binary vectors and the set of all the variables in (5). The numerator in (6) is a regularized likelihood function based on the shared distribution (i.e., the proposed 2L-WMM) for labeled and unlabeled PolSAR data. $\lambda_{\mathfrak{U}}$ and $\lambda_{\mathfrak{L}}$ are two positive balance parameters.

Following the variational inference, all the update equations are derived in closed form as

$$\alpha_i = \alpha_{i0} + \sum_{n \in \mathfrak{U}} \lambda_{\mathfrak{U}} \mathbf{E}[z_{ni}] + \sum_{m \in \mathfrak{L}} \lambda_{\mathfrak{L}} \mathbf{E}[z_{mi}], \tag{7a}$$

$$\beta_{ij} = \beta_{ij0} + \sum_{n \in \mathfrak{U}} \lambda_{\mathfrak{U}} r_{nij} + \sum_{m \in \mathfrak{L}} \lambda_{\mathfrak{L}} r_{mij}, \tag{7b}$$

$$\eta_{ij} = \eta_{ij0} + \sum_{n \in \mathfrak{U}} L\lambda_{\mathfrak{U}} r_{nij} + \sum_{m \in \mathfrak{L}} L\lambda_{\mathfrak{L}} r_{mij}, \tag{7c}$$

$$W_{ij} = \frac{1}{\eta_{ij}}\{\eta_{ij0}W_{ij0} + \sum_{n \in \mathfrak{U}} L\lambda_{\mathfrak{U}} r_{nij}C_n + \sum_{m \in \mathfrak{L}} L\lambda_{\mathfrak{U}} r_{mij}C_m\}, \tag{7d}$$

where $r_{nij} = \mathbf{E}[z_{ni}]\mathbf{E}[y_{nij}]$ and r_{mij} takes the same form as r_{nij}. $\mathfrak{U}$ and $\mathfrak{L}$ are the index set of the labeled and unlabeled data, and

$$\mathbf{E}[y_{nij}] = \frac{\exp(\mathbf{E}[\ln(\omega_{ij}\mathcal{W}(C_n; L, \Omega_{ij}))])}{\sum_{k=1}^K \exp(\mathbf{E}[\ln(\omega_{ik}\mathcal{W}(C_n; L, \Omega_{ik}))])}. \tag{8}$$

To incorporate the local correlation and alleviate the "salt-and-pepper" appearance in the classification results, a MRF prior $p(z_{ni} = 1|l_{\partial_n}; \gamma)$ is imposed on the indicator variable $\mathbf{z}_{ni}$, which is thus updated for the unlabeled data by

$$\mathbf{E}[z_{ni}] \propto p(z_{ni} = 1|l_{\partial_n}; \gamma) \cdot \exp(\mathbf{E}[\ln \phi_i])$$
$$\cdot \exp(\mathbf{E}[\sum_{j=1}^K \ln(\omega_{ij}^{y_{nij}}\mathcal{W}^{y_{nij}}(C_n; L, \Omega_{ij}))]). \tag{9}$$

The multiple subcategories in a complicated category is explicitly considered by the term of summation over K subcomponents in (9). For labeled pixel m belonging to the i-th category, $\mathbf{E}[z_{mi}] = 1$ and $\mathbf{E}[z_{mj}] = 0$ for $j \neq i$. In (9), ∂_n is the neighborhood of pixel n, and γ is the inverse temperature parameter to control the smoothness in the classification

(a)　　　　(b)　　　　(c)

(d)　　　　(e)　　　　(f)

(g)　　　　　　　　(h)
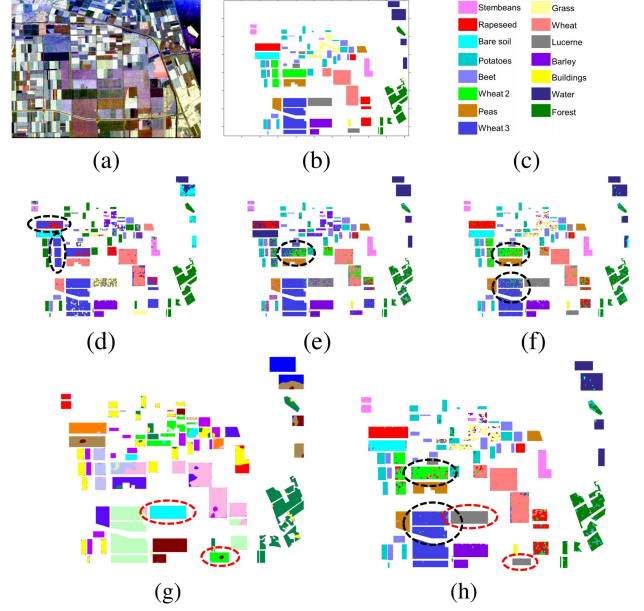
Fig. 1. The realistic PolSAR image and the classification maps. (a) The Pauli RGB image of Flevoland data set. (b) The ground truth. (c) The color codes. (d) The unsupervised version of the proposed model. (e) The supervised version of the proposed model. (f) The semi-supervised version of the proposed model without considering spatial interdependencies. (g) The RSS method [8]. (h) The proposed method.

results. In the proposed method, the introduced spatial prior takes the form of

$$p(z_{ni} = 1|l_{\partial_n}; \gamma) = \frac{\exp(\gamma \sum_{m \in \partial_n} \delta(l_m, i))}{\sum_{j=1}^M \exp(\gamma \sum_{m \in \partial_n} \delta(l_m, j))}, \tag{10}$$

where l_{∂_n} includes the labels of all neighbors of pixel n, and l_m is the label for the neighbor m. $\delta(l_m, i) = 1$ if $l_m = i$; otherwise, $\delta(l_m, i) = 0$. In each iteration, the label is updated by $l_n = \arg\max_i \mathbf{E}[z_{ni}], n \in \mathfrak{U}$. According to this criterion, the classification map can be conveniently obtained.

By alternatively implementing (8), (9), and (7a)-(7d) until the stop criterion is reached, the proposed model can be learned with all equations updating in a closed form.

4. EXPERIMENTAL RESULTS AND DISCUSSION

The proposed method is tested based on a realistic PolSAR image acquired by NASA/JPL AIRSAR over Flevoland, the Netherlands. This image with the size of 750×1024 includes buildings, water, and various types of crops.

The proposed method is evaluated against the unsupervised version of the proposed model, the supervised version of the proposed model, the semi-supervised version of the proposed model without considering the spatial interdependencies, and an existing semi-supervised method (i.e., the

robust semi-supervised (RSS) classification method [8]) in terms of both qualitatively and quantitatively. To train these models, 1% of the labeled samples are randomly selected for each category. The number of training samples for a category ranges from 7 to 211, which depends on the total number of labeled samples in a category. The metrics for quantitative evaluation include the producer's accuracy, the overall accuracy (OA), and the kappa coefficient (κ). For the unsupervised version, the set of metrics corresponding to the highest OA in 10 independent tests is presented in Table 1. For the remaining methods, the average of the metric values over 10 independent tests are reported. In Table 1, unrecognized categories are indicated by "–". Since we cannot find the code for the RSS method, its classification map in Fig. 1 and metric values in Table 1 are from [8].

According to Fig. 1(d) and the ground truth in Fig. 1(b), the unsupervised version of the proposed model fails to assign the pixels in the upper black circles to the same category, and misclassified pixels are observed. This misclassification is corrected by the semi-supervised version of the proposed model without considering the spatial interdependencies [see Fig. 1(f)], implying the effectiveness of the proposed method in incorporating label information to guide the classification. The proposed method further improves the classification performance by introducing the spatial interdependencies, which is confirmed by its larger OA and κ in Table 1.

With only 1% of labels (ranging from 7 to 211 labels for a category), the supervised version of the proposed model fails to achieve an accurate classification, in view of the misclassification in the black circle of Fig. 1(e) and its smaller OA in the second column of Table 1. In contrast, as shown in the third and the last column of Table 1, both the semi-supervised version of the proposed model without MRF and the proposed semi-supervised method achieve better performance due to the incorporation of the unlabeled samples.

In the result for the RSS method [see Fig. 1(g)], the areas in the red circles are classified as two separate categories, which is different from the ground truth. This observation implies the obvious misclassification for the RSS method. In contrast, the proposed method achieves the consistent result with the ground truth according to Fig. 1(h) and Table 1.

5. CONCLUSION

A two-level Wishart mixture model with MRF has been proposed for semi-supervised classification of the PolSAR images. Within the framework of finite mixture models, WMMs were introduced as the component densities (rather than a unimodal distribution). This modeling scheme facilitated modeling subcategories in classification tasks. To alleviate the "salt-and-pepper" effect, the MRF prior was introduced to incorporate the spatial interdependencies. The variational learning algorithm for the proposed model was achieved with all the closed-form updates. The experimental results demon-

Table 1. Classification Accuracy with the Flevoland Data Set.

Class	Producer's Accuracy (%)				
	Unsupervised Version	Supervised Version	Semi-supervised Version without MRF	Semi-supervised RSS	Proposed
Stembeans	77.57	84.38	95.09	54.00	**97.12**
Rapeseed	25.92	40.13	77.26	46.00	**86.37**
Bare soil	96.29	01.01	97.49	95.00	**98.86**
Potatoes	–	84.24	86.45	83.00	**95.04**
Beet	85.94	78.16	89.22	**99.00**	97.75
Wheat 2	–	41.42	70.22	70.00	**81.28**
Peas	–	81.71	92.89	96.00	**97.61**
Lucerne	34.68	59.06	93.42	70.00	**97.06**
Wheat 3	94.79	**98.21**	92.07	98.00	97.25
Grass	38.87	03.02	75.18	60.00	**85.35**
Barley	97.68	93.14	91.82	**100.00**	96.68
Wheat	76.47	67.53	86.62	91.00	**94.32**
Buildings	00.48	80.92	86.84	35.00	**87.23**
Forest	**98.93**	77.42	82.13	94.00	88.09
Water	38.93	94.08	91.64	59.00	**94.23**
OA (%)	55.28	69.78	86.67	81.00	**93.13**
κ	0.5067	0.6687	0.8546	0.8000	**0.9251**

strated the effectiveness of the proposed method in incorporating both the label information and the spatial interdependencies.

6. REFERENCES

[1] J.-S. Lee and E. Pottier, *Polarimetric Imaging: From Basics to Applications*, CRC Press, Boca Raton, FL, 2009.

[2] J.-S. Lee, M. R. Grunes, T. L. Ainsworth, L. J. Du, D. L. Schuler, and S. R. Cloude, "Unsupervised classification using polarimetric decomposition and the complex Wishart classifier," *IEEE Trans. Geosci. Remote Sens.*, vol. 37, no. 5, pp. 2249–2258, Sep. 1999.

[3] X. Deng, C. López-Martínez, J. S. Chen, and P. P. Han, "Statistical modeling of polarimetric SAR data: A survey and challenges," *Remote Sensing*, vol. 9, no. 4, pp. 348, 2017.

[4] Y. H. Wu, K. Ji, W. Yu, and Y. Su, "Region-based classification of polarimetric SAR images using Wishart MRF," *IEEE Geosci. Remote Sens. Lett.*, vol. 5, no. 4, pp. 668–672, Oct. 2008.

[5] W. Song, M. Li, P. Zhang, Y. Wu, X. Tan, and L. An, "Mixture WGΓ -MRF model for PolSAR image classification," *IEEE Trans. Geosci. Remote Sens.*, vol. 56, no. 2, pp. 905–920, Feb. 2018.

[6] N. R. Goodman, "Statistical analysis based on a certain multivariate complex Gaussian distribution (an introduction)," *Ann. Math. Statist.*, vol. 34, no. 1, pp. 152–177, Mar. 1963.

[7] C. M. Bishop, *Pattern Recognition and Machine Learning*, Springer-Verlag, New York, 2006.

[8] B. Hou, Q. Wu, Z. Wen, and L. Jiao, "Robust semisupervised classification for PolSAR image with noisy labels," *IEEE Trans. Geosci. Remote Sens.*, vol. 55, no. 11, pp. 6440–6455, Nov. 2017.